$P\rho Tx$ Measurements for Gas-Phase Pentafluoroethane + Propane Mixtures by the Burnett Method[1]

Yohei Kayukawa[2,3] and Koichi Watanabe[2]

1. Paper to be presented at the Fourteenth Symposium on Thermophysical Properties, June 25-30, 2000, Boulder, Colorado, U.S.A.
2. Department of System Design Engineering, Faculty of Science and Technology, Keio University, 3-14-1, Kohoku-ku, Yokohama 223-8522, Japan
3. To whom correspondence should be addressed.

ABSTRACT

In some refrigeration-based applications, hydrocarbons (HCs) are expected to be promising long-term alternative refrigerants because of their zero ODP and negligible GWP values. But there exists a serious disadvantage that they are flammable. In spite of their flammability, however, commercial demands for HCs are increasing not only in several European countries but also in southeast Asia. On the other hand, the flammability is considered a fatal issue in U.S.A. and Japan. In order to suppress the flammability, blended mixtures of HC with nonflammable HFCs are considered. As one of such mixtures, pentafluoroethane (R-125) and propane (R-290) mixtures are dealt with in the present study. Although the thermodynamic properties of each single component have been studied rather extensively, there is no study reported on those of this binary system. Accordingly, we aimed to measure the gas-phase $P\rho Tx$ properties of the binary R-125(1) + R-290(2) systems by using the Burnett isothermal-• isochoric coupling method. The present measurements cover an extensive range of temperatures 305-380 K, pressures up to 4.5 MPa, and densities up to 2.5 mol/dm^{-3} for the binary systems with 4 different mole fractions of x_1=0.00, 0.29, 0.50 and 0.75, respectively. The present paper discusses the gas-phase $P\rho Tx$ properties for the first time regarding the present binary mixtures at their entire compositions.

KEYWORDS: Binary refrigerant mixtures; Burnett method; gas-phase $P\rho Tx$ properties; natural refrigerant; pentafluoroethane; propane; R-125; R-290.

Introduction

In conjunction with an increasing concern about the global warming impact by the hydrofluorocarbon (HFC) refrigerants which have been proposed being promising alternative refrigerants to replace several conventional chlorofluorocarbon (CFC) and/or hydrochlorofluorocarbon (HCFC) refrigerants, the refrigeration-based industries worldwide are facing another important issue to identify the long-term and environmentally-benign alternatives.

Among the possible candidates along this line, there exists a possibility to blend the hydrocarbon (HC) refrigerants with some selected HFC compounds. Namely, an essential drawback of the flammability issue of HCs is expected to be reduced significantly by blending them with nonflammable HFCs, whereas considerable global warming potential (GWP) of HFCs would be reduced by blending with HCs that have negligible GWP values. In the present study, therefore, we aimed to conduct a series of the gas-phase $P\rho Tx$ property measurements for the binary R-125 (1) + R-290 (2) mixtures by the Burnett isothermal-isochoric coupling method. The present measurements cover an extended range of temperatures 305–380 K, and pressures up to 4.5 MPa, at 4 different compositions including pure R-290 component.

Based on the measurements, we have also developed a simple truncated virial equation of state, and the thermodynamic behavior including the temperature dependence of the second virial coefficients calculated from the present model has also been discussed in this paper.

Experimental

Figure 1 shows a schematic diagram of the experimental setup for the Burnett isotherm-isochoric coupling method. The apparatus consists of four subsystems; a cell system, a sample filling system, a temperature control/measuring system and a pressure control/measuring system.

The cell system consists of two cells, a sample cell (A) and an expansion vessel (B), and a constant-volume valve (V1) connecting two cells. Both cells are thick walled spherical vessels made of SUS-304. The inner volume of the vessel is approximately 500 cm^3 for the sample cell, whereas 250 cm^3 for the expansion vessel. The cell constant, N, which is equivalent to the inner volume ratio of the two cells at zero pressure, is an essential factor to determine the density and the compressibility factor. It was precisely determined by using gaseous helium being N=1.50105 ± 0.00010, since its $P\rho T$ properties are well known.

A variable-volume vessel with the metallic bellows (T) is a main part of the sample filling subsystem. Since the sample composition is one of the important properties of the mixtures, we paid a full attention in a preparation process of the mixture sample as well as in its charging into the sample cell. Namely, the mixture sample with a known initial composition was prepared in a supplying vessel in advance, and then transferred to a sample-charging variable-volume vessel (T) with the metallic bellows. By filling high pressure nitrogen gas at about 3 MPa inside the bellows, the sample outside was maintained at compressed-liquid phase. Then, the specified quantity of sample was introduced into the sample cell little by little by opening the valve V2 simultaneously, so that there assumed no composition change might be observed before and after the filling.

Regarding the temperature measurements, we assumed that the sample

temperature is equivalent to the thermostated bath-fluid (silicone oil) temperature being in thermodynamic equilibrium within a fluctuation of ±3 mK. A main heater (G) was used to increase the temperature, whereas a subheater (F) was used for controlling the temperature at the prescribed level. The subheater was controlled by a PID controller (R) according to the detected temperature by a standard platinum resistance thermometer (D) installed in the vicinity of the sample cell.

After confirming temperature stability, the sample pressure was measured with a differential pressure transducer (C) and quartz pressure transducers (L & M) at this state 1. We have used nitrogen gas as a pressure transferring medium in the differential pressure transducer and the pressure difference between the sample and nitrogen gas has to be carefully calibrated in advance as a function of temperature.

Note that we have successfully used the present Burnett apparatus to measure the thermodynamic properties of various refrigerants and their mixtures up to the present. Some of the recent publications similar to the present study include that for R-32 by Qian *et al.*[1], R-125 by Ye *et al.* [2], R-236ea[3], R-143a[4], and the binary R-32 + R-125[5] and R-125 + R-143a[6] by Zhang *et al.*, and the ternary mixture R-32 + R-125 + R-143a by Tada *et al.*[7] and Kayukawa *et al.*[8]

According to the ISO recommendation[9], the experimental uncertainties were estimated in terms of the expanded uncertainty with the coverage factor, being k=2. The estimated uncertainties are not greater than ±7 mK in temperature, ±0.8 kPa in pressure, ±0.1% in density, and ±0.1 mol% in composition, respectively. Regarding the sample preparation, each single-component sample was blended on the mass-basis, and they have research grade purities, i.e., 99.953 mass% for R-125, and 99.9 mol% for propane, respectively. These sample purities are those analyzed by the chemical

manufacturers and we did not add any further purification.

Experimental Results

A total of 187 $P\rho Tx$ properties of the binary R-125(1) + R-290(2) mixtures in their gaseous phase have been obtained in an extensive range of temperatures 305–380 K, and pressures up to 4.9 MPa, at 4 different compositions with the mole fraction of R-125, x_1 = 0.00, 0.288, 0.500 and 0.750. They consist of the measurements along 6 isochores for pure R-290, those along 9 isochores for the mixture with x_1= 0.288, those along 10 isochores with x_1 = 0.500, and those along 10 isochores with x_1 = 0.750, respectively. They all are tabulated in Table 1, where the compressibility factor, Z, besides molar density, ρ, are given at respective temperatures and pressures for 4 different compositions. Figure 2 illustrates a data distribution of these present measurements on a pressure-temperature diagram where the vapor-pressure curve for each pure component calculated from REFPROP (ver. 6.01)[10] is also included.

Discussion

Based on the present measurements, a thermodynamic model which represents the gas-phase $P\rho Tx$ properties of the binary R-125(1) + R-290(2) system in its entire range of compositions was developed. The present model is expressed as a truncated virial equation of state, for the compressibility factor, Z, as given below, where ρ denotes the molar density.

$$Z = 1 + \sum_{i}^{2}\sum_{j}^{2} x_i x_j B_{ij}\rho + \sum_{i}^{2}\sum_{j}^{2}\sum_{k}^{2} x_i x_j x_k C_{ijk}\rho^2 + \sum_{i}^{2} x_i D_i \rho^3 \qquad (1)$$

Note that the relations $B_{ij} = B_{ji}$ and C_{ijk}=C_{ikj}=C_{jik}=C_{jki}=C_{kij}=C_{kji} exist, since B_{ij} denotes the second virial coefficient based on the intermolecular potential of component i and component j, whereas C_{ijk} represents the third virial coefficient based on that of component i, j and k. When $i = j = k$, then B_{ij} or C_{ijk} is equivalent to the second and third virial coefficient for pure component, or they denote the excess second or third virial coefficient of two different components. Both B_{ij} and C_{ijk} are expressed as functions of the reduced temperature, $T_r = T/T^*$, given in eqs. 2 and 3, respectively.

$$B_{ij} = b_{1,ij} + b_{2,ij} T_r^{-1} + b_{3,ij} \exp\left(T_r^{-1}\right), \qquad (2)$$

$$C_{ijk} = c_{1,ijk} + c_{2,ijk} T_r^{-k_{1,ijk}} + c_{3,ijk} T_r^{-k_{2,ijk}} \qquad (3)$$

It should also be noted that the characteristic temperature, T^*, which is equivalent to the critical temperature, $T_{C,i}$, for pure component, is defined in eq. 4 and 5 for the excess second and third virial coefficient, respectively, by employing the critical temperature values being 339.165 K[12] for $T_{C,1}$ and 369.825 K[13] for $T_{C,2}$.

$$T^* = \sqrt{T_{C,i} T_{C,j}} \qquad (4)$$

$$T^* = \sqrt[3]{T_{C,i} T_{C,j} T_{C,k}} \qquad (5)$$

The functional form of eq. 2 for the second virial coefficient was originally formulated by Zhang *et al.*[11] of our group for several HFC mixtures, whereas we have applied a conventional form for the third virial coefficient as given in eq. 3.

Note that the fourth term with D_i in eq. 1 is expressed as a simple cubic function of reduced temperature as given in eq. 6. Since the present model is the simple truncated virial formulation without taking into account the fourth and higher virial terms, a simplified mole-fraction average correlation for coefficient D was used for each pure component.

$$D_i = d_i T_r^{-3} \tag{6}$$

B_{11}, C_{111} and D_1 represent the contribution of the pure component R-125, and their numerical constants were obtained by the present authors[14] based on their analysis of the Burnett measurements of Ye *et al.*[2] We have simply employed these numerical constants in the present modeling. On the other hand, the numerical constants which appear in eqs. 2, 3 and 4 for B_{22}, C_{222} and D_2 which represent R-290 have been optimized and determined by means of our own least-squares fitting to the present measurements for R-290. The effectiveness of the representations for R-290 will be discussed later. We have then obtained the numerical constants for the excess virial coefficients, B_{12}, C_{112} and C_{122}, by means of the same optimum fitting procedure of eq. 1 to the present measurements for the binary R-125 (1) +R-290 (2) mixtures, at 3 different compositions. All of these numerical constants thus determined in the present study are tabulated in Table 2.

Figure 3 shows the relative pressure deviations, from the present measured results for R-290. For the purpose of simplicity to compare the present experimental data with available models including the present equation of state, eq. 1, the Helmholtz model recently proposed by Miyamoto and Watanabe[15] and the prediction by REFPROP (ver. 6.01)[10] for pure R-290, the base line in Figure 3 corresponds to the present data, while the ΔP values denote the pressure deviations of the calculated pressure values by different models mentioned above. It is obvious that the present model represents the measured $P\rho Tx$ properties with an excellent reproducibility within ±0.13% in pressure. The present experimental $P\rho Tx$ properties deviate from those calculated from REFPROP by –0.28% to +0.25% in pressure, whereas those of the Miyamoto and Watanabe model from the present data are from –0.18% up to +0.28%. This fact confirms a satisfactory reliability of the present measurements as well as the present thermodynamic model for pure R-290. The temperature dependence of the second virial coefficient for R-290 will be discussed later, together with those for the binary R-125(1) + R-290(2) mixture.

Figure 4 illustrates a similar comparison in terms of the relative pressure deviation of the calculated pressure values by eq. 1 and the prediction of the REFPROP from the present data for the binary R-125(1) + R-290(2) mixture. It is apparent that the present model shows an excellent reproducibility of the present experimental data with x_1 = 0.500 and 0.750 within ±0.39% in pressure, while its representation at lower density data for the mixture with x_1 = 0.288 deviate by +0.69% in maximum. The predicted values from the REFPROP deviate larger than our model, almost within ±1% in pressure, but the deviations become more significant at higher densities.

Figure 5 shows the temperature dependence of the calculated second virial

coefficients, B_{11} and B_{22}, and the excess virial coefficient, B_{12}. The caluculated B_{22} and B_{12} values reported by McElroy[16] are also included in this figure. It is found that the second virial coefficients exhibit thermodynamically sound behavior with temperature. The excess virial coefficient, B_{12}, has larger value than those both of R-125 and R-290, and this fact suggests that the present binary system exhibit a typical strong positive pressure azeotrope. The B_{22} and B_{12} values by McElroy agree well with those calculated from the present model within ±3.3% for B_{22} and ±3.7% for B_{12}, respectively. Our experimental values of the mixed second virial coefficient, B_m, that were determined by extrapolating the $(Z\text{-}1)/\rho$ values to the zero density, are shown at different temperatures in Figure 6 together with the curves calculated from the conventional mixing-rule such as appeared in eq. 1. It is obvious that the present experimental values are well represented by the present model. The relative deviations of these experimental second virial coefficient values from our model are illustrated in Figure 7, and it is apparent that the experimental second virial coefficients are well represented within 0.0 - +0.4% for pure R-290 and 0.0 - +0.2% for the mixtures. The reproducibility of the present model for the mixtures is better than that for pure R-290, since we could not obtain an enough number of isothermal data for R-290 to determine the experimental second virial coefficient precisely. Because of the page limitation, we excluded the discussion on the third virial coefficient as well as thermodynamic behavior of the derived properties, but the present model did also an excellent job to represent their thermodynamically consistent behaviors as far as the present measured range of temperatures is concerned.

Conclusion

A total of 187 gas-phase $P\rho Tx$ properties for the binary R-125 (1) + R-290 (2) system have been reported for the extensive range of temperatures and pressures at 4 different compositions. This is the first set of data ever reported for the gas-phase $P\rho Tx$ properties of this binary refrigerant system. On the basis of the present measurements, the thermodynamic model was developed. The model represents our experimental $P\rho Tx$ properties and the virial coefficents for the present binary system including pure components with sufficient accuracy. The developed model has been confirmed to provide the thermodynamically consistent representation for the binary system of the present interest.

Literature Cited

(1) Qian, Z.-Y.; Sato, H.; Watanabe, K. Compressibility Factors and Virial Coefficients of Difluoromethane (HFC-32) Determined by Burnett Method. *JSME Int. J.*, **1993**, 36, 665-670.

(2) Ye, F.; Sato, H.; Watanabe, K. Gas-phase *PVT* Properties and Vapor Pressures of Pentafluoroethane (HFC-125) Determined According to the Burnett Method. *J. Chem. Eng. Data* **1995**, *40, 1*, 148-152.

(3) Zhang, H.-L.; Sato, H.; Watanabe, K. Vapor Pressure Measurements of 1,1,1,2,3,3-Hexafluoropropane from 300 to 410 K. *J. Chem. Eng. Data* **1995**, *40*, 1281-1284.

(4) Zhang, H.-L.; Sato, H.; Watanabe, K. Vapor Pressures, Gas-phase *PVT* Properties and Second Virial Coefficients for 1,1,1-Trifluoroethane. *J. Chem. Eng. Data* **1995**, *40*, 887-890.

(5) Zhang, H.-L.; Sato, H.; Watanabe, K. Gas Phase *PVT* Properties for the Difluoroethane + Pentafluoroethane (R-32 + 125) System. *J. Chem. Eng. Data* **1996**, *41*, 1401-1406.

(6) Zhang, H.-L.; Sato, H.; Watanabe, K. *PVTx* Properties in the Gas Phase for Binary R-125/143a System. *Fluid Phase Equil*. **1998**, *150*, 333-341.

(7) Tada, S.; Zhang, H.-L.; Sato, H.; Watanabe, K. Mesurements of Gas-phase *PVTx* Properties of the Ternary R-32/125/143a Mixture. *Proc. of the 5th Asian Thermophysical Properties Conference*, Seoul, Korea **1998**, 269-272.

(8) Kayukawa, Y.; Tada, S.; Zhang, H.-L.; Watanabe, K. Mesurements of Gas-phase *PVTx* Properties for the Ternary R-32/125/143a Mixture. Paper presented at *the 20th Int. Congress of Refrig*eration, Sydney, Australia **1998**.

(9) International Organization of Standardization. Guide to the Expression of Uncertainty in Measurement; ISO: Switzerland, 1993

(10) McLinden, M. O.; Kein, S. A.; Lemmon, E. W.; Peskin, A. P. REFPROP, Thermodynamic and Transport Properties of Refrigerants and Refrigerant Mixtures. Standard Reference Database 23 – Version 6.01, NIST: U. S. Secretary of Commerce on behalf of the United States of America, 1998.

(11) Zhang, H.-L.; Sato, H.; Watanabe, K. Second Virial Coefficients for R-32, R-125, R-143a, R-152a and Their Binary Mixtures, *Proc. of the 19th Int. Congress of Refrig*, The Hague, The Netherland **1995**, • *a*, 622-629.

(12) Kuwabara, S.; Aoyama, H.; Sato, H.; Watanabe, K. Vapor-Liquid Coexistence Curve in the Critical Region and the Critical Temperatures and Densities of Difluoroethane and Pentafluoroethane, *J. Chem. Eng. Data* **1995**, *40*, 112-116.

(13) Thomas, R. H. P.; Harrison, R. H. Pressure-Volume-Temperature Relations of

Propane, *J. Chem. Eng. Data* **1982,** *27***,** 1.

(14) Kayukawa, Y.; Watanabe, K. Thermodynamic Modeling of the Gas-Phase *PVTx* Properties for the Ternay R-32/125/143a System. Paper to be presented at *the Fourteenth Symp. on Thermophys. Prop*., Boulder, Colorado, U. S. A., **2000**.

(15) Miyamoto, H. and Watanabe, K., A Thermodynamic Model for Fluid-phase Propane, Paper to be submitted to *Int. J. Thermophys*. **2000**

(16) McElroy, P. J., Excess and Unlike-Interaction 2nd Virial-Coefficients and Excess Molar Enthalpy of a Refrigerant Mixture ($0.500CH_2FCF_3$ + $0.500C_3H_8$). *J. Chem. Thermodyn.* **1995**, *27*, 1047-1052

Table. 1 Experimental $P\rho Tx$ Properties for R-125(1) + R-290(2) Mixtures

T/K	P/kPa	ρ /mol•dm^{-3}	Z
	x_1=0.00		
380.000	3814.9	1.929	0.6263
380.000	2980.5	1.285	0.7335
380.000	2204.9	0.8560	0.8142
380.000	1573.1	0.5703	0.8724
380.000	1095.7	0.3799	0.9133
380.000	751.8	0.2531	0.9415
365.000	3447.5	1.930	0.5892
365.000	2763.5	1.286	0.7084
365.000	2073.6	0.8566	0.7973
365.000	1491.7	0.5707	0.8611
365.000	1044.2	0.3802	0.9057
365.000	718.9	0.2533	0.9363
350.000	2539.6	1.287	0.6789
350.000	1939.3	0.8572	0.7774
350.000	1408.8	0.5711	0.8477
350.000	991.8	0.3805	0.8967
350.000	685.3	0.2535	0.9303
335.000	1803.3	0.8579	0.7538
335.000	1324.4	0.5715	0.8318
335.000	939.0	0.3807	0.8860
335.000	651.5	0.2537	0.9232
320.000	1238.1	0.5719	0.8128
320.000	885.4	0.3810	0.8733
320.000	617.4	0.2538	0.9147
305.000	830.5	0.3813	0.8579
305.000	582.6	0.2540	0.9044
	x_1=0.288		
380.000	4397.6	2.137	0.6513
380.000	3377.8	1.424	0.7485
380.000	2474.6	0.9485	0.8236
380.000	1756.4	0.6319	0.8784
380.000	1221.5	0.4210	0.9171
380.000	836.6	0.2805	0.9440
380.000	567.9	0.1869	0.9623
380.000	382.8	0.1245	0.9747
380.000	257.1	0.08293	0.9831
365.000	3984.9	2.139	0.6139
365.000	3132.2	1.425	0.7226
365.000	2322.8	0.9492	0.8058
365.000	1664.4	0.6324	0.8663
365.000	1163.1	0.4213	0.9090
365.000	799.3	0.2807	0.9385
365.000	543.4	0.1870	0.9586
365.000	366.7	0.1246	0.9723
365.000	246.3	0.08299	0.9814
350.000	3557.8	2.140	0.5705
350.000	2912.6	1.426	0.6925
350.000	2171.8	0.9499	0.7851
350.000	1571.2	0.6329	0.8523
350.000	1104.2	0.4216	0.8995
350.000	761.5	0.2809	0.9321
350.000	518.9	0.1871	0.9544
350.000	350.6	0.1247	0.9694
350.000	237.1	0.08305	0.9795
335.000	3022.1	2.142	0.5195
335.000	2619.4	1.427	0.6573
335.000	2017.4	0.9506	0.7611
335.000	1476.6	0.6333	0.8359
335.000	984.6	0.4219	0.8885
335.000	723.6	0.2811	0.9247
335.000	494.2	0.1873	0.9494
335.000	334.5	0.1248	0.9661
335.000	225.0	0.08311	0.9773
320.000	2210.6	1.428	0.6153
320.000	1858.6	0.9513	0.7325
320.000	1379.8	0.6338	0.8166
320.000	984.4	0.4222	0.8755

Table. 1 (continued)

T/K	P/kPa	ρ /mol•dm^{-3}	Z
320.000	685.3	0.2813	0.9160
320.000	469.5	0.1874	0.9436
320.000	318.3	0.1248	0.9622
320.000	214.3	0.08317	0.9747
305.000	1546.9	0.9520	0.6981
305.000	1280.4	0.6342	0.7935
305.000	923.1	0.4225	0.8600
305.000	646.5	0.2815	0.9056
305.000	444.5	0.1875	0.9366
305.000	302.1	0.1249	0.9576
305.000	203.7	0.08323	0.9716
x_1=0.500			
380.000	4917.4	2.454	0.6352
380.000	3779.6	1.635	0.7335
380.000	2785.8	1.089	0.8117
380.000	1988.1	0.7257	0.8697
380.000	1387.4	0.4835	0.9110
380.000	954.5	0.3221	0.9397
380.000	651.2	0.2146	0.9594
380.000	439.9	0.1430	0.9727
380.000	295.7	0.09524	0.9818
380.000	198.6	0.06345	0.9878
365.000	4429.2	2.456	0.5954
365.000	3490.4	1.636	0.7050
365.000	2611.5	1.090	0.7917
365.000	1880.9	0.7262	0.8559
365.000	1320.5	0.4838	0.9016
365.000	911.9	0.3223	0.9334
365.000	623.2	0.2147	0.9551
365.000	421.3	0.1431	0.9699
365.000	283.7	0.09531	0.9798
365.000	190.4	0.06350	0.9865
350.000	3926.7	2.458	0.5495
350.000	3194.1	1.637	0.6721
350.000	2434.0	1.091	0.7688
350.000	1772.1	0.7268	0.8401
350.000	1252.8	0.4842	0.8909
350.000	869.7	0.3226	0.9261
350.000	595.0	0.2149	0.9503
350.000	403.1	0.1432	0.9666
350.000	271.7	0.09538	0.9777
350.000	182.6	0.06354	0.9851
335.000	3400.6	2.460	0.4955
335.000	2887.5	1.639	0.6338
335.000	2252.0	1.092	0.7421
335.000	1661.4	0.7273	0.8219
335.000	1183.7	0.4845	0.8785
335.000	825.7	0.3228	0.9177
335.000	566.7	0.2150	0.9446
335.000	384.7	0.1433	0.9629
335.000	259.6	0.09545	0.9751
335.000	174.6	0.06359	0.9834
320.000	2064.4	1.092	0.7106
320.000	1548.0	0.7278	0.8004
320.000	1113.4	0.4849	0.8639
320.000	781.3	0.3230	0.9079
320.000	538.0	0.2152	0.9380
320.000	366.0	0.1434	0.9584
320.000	247.4	0.09551	0.9722
320.000	166.5	0.06363	0.9814
305.000	1431.7	0.7283	0.7747
305.000	1041.7	0.4852	0.8466
305.000	736.5	0.3232	0.8963
305.000	509.1	0.2153	0.9303
305.000	347.4	0.1435	0.9533
305.000	235.1	0.09558	0.9687
305.000	158.5	0.06368	0.9791
x_1=0.750			
380.000	4672.6	2.225	0.6645
380.000	3536.5	1.471	0.7583

Table. 1 (continued)

T/K	*P*/kPa	ρ /mol•dm^{-3}	*Z*	*T*/K	*P*/kPa	ρ /mol•dm^{-3}	*Z*
380.000	2577.8	0.9803	0.8303	350.000	163.7	0.05719	0.9866
380.000	1825.8	0.6531	0.8831				
380.000	1267.2	0.4351	0.9204	335.000	3320.6	2.230	0.5354
380.000	866.4	0.2899	0.9462	335.000	2739.7	1.475	0.6658
380.000	587.4	0.1931	0.9638	335.000	2099.4	0.9825	0.7656
380.000	396.2	0.1287	0.9757	335.000	1532.1	0.6545	0.8386
380.000	266.2	0.08571	0.9838	335.000	1082.9	0.4361	0.8901
380.000	177.8	0.05710	0.9892	335.000	749.2	0.2905	0.9257
				335.000	511.7	0.1935	0.9501
365.000	4236.6	2.227	0.6276	335.000	346.8	0.1289	0.9665
365.000	3278.2	1.473	0.7318	335.000	233.9	0.08590	0.9776
365.000	2421.5	0.9810	0.8117	335.000	156.6	0.05723	0.9850
365.000	1729.2	0.6536	0.8703				
365.000	1206.5	0.4354	0.9117	320.000	1931.4	0.9832	0.7365
365.000	828.2	0.2901	0.9403	320.000	1430.4	0.6550	0.8186
365.000	562.4	0.1933	0.9598	320.000	1019.7	0.4364	0.8766
365.000	379.7	0.1288	0.9731	320.000	709.6	0.2907	0.9166
365.000	255.4	0.08578	0.9820	320.000	486.2	0.1937	0.9440
365.000	170.8	0.05714	0.9880	320.000	330.2	0.1290	0.9624
				320.000	223.0	0.08596	0.9749
350.000	3788.1	2.228	0.5851	320.000	149.6	0.05727	0.9832
350.000	3013.2	1.474	0.7013				
350.000	2262.3	0.9818	0.7903	305.000	1755.4	0.9838	0.7016
350.000	1631.5	0.6541	0.8556	305.000	1325.8	0.6554	0.7950
350.000	1145.1	0.4357	0.9016	305.000	955.5	0.4367	0.8607
350.000	788.7	0.2903	0.9335	305.000	669.2	0.2909	0.9059
350.000	537.1	0.1934	0.9553	305.000	460.3	0.1938	0.9368
350.000	363.3	0.1288	0.9700	305.000	313.4	0.1291	0.9576
350.000	244.7	0.08584	0.9800	305.000	211.8	0.08602	0.9717

Table 2. Numerical Constants in eqs. 2, 3 and 6

ij	$b_{1,ij}$/dm^3·mol^{-1}	$b_{2,ij}$/dm^3·mol^{-1}	$b_{3,ij}$/dm^3·mol^{-1}
11	4.229178×10^{-1}	1.170954×10^{-1}	-2.979276×10^{-1}
22	2.622157×10^{-1}	4.636876×10^{-1}	3.593101×10^{-1}
12	3.133964×10^{-1}	-4.173097×10^{-4}	1.901441×10^{-1}

ijk	$c_{1,ijk}$/dm^6·mol^{-2}	$c_{2,ijk}$/dm^6·mol^{-2}	$c_{3,ijk}$/dm^6·mol^{-2}	$k_{1,ijk}$	$k_{2,ijk}$
111	8.218857×10^{-4}	2.697741×10^{-2}	-1.737623×10^{-3}	3	13
222	2.101379×10^{-2}	1.115478×10^{-2}	-6.818215×10^{-3}	7.5	9
112	-6.488578×10^{-3}	3-23620$\times10^{-2}$	-1.926943×10^{-3}	3	11
122	1.557639×10^{-2}	1.382724×10^{-2}	-5.251839×10^{-3}	6	9

i	d_i/dm^9·mol^{-3}
1	-2.287655×10^{-4}
2	-1.202654×10^{-3}

Figure Captions

Figure 1. Schematic diagram of the experimental Burnett apparatus: (A) sample cell; (B) expansion cell; (C) differential pressure transducer; (D) platinum resistance thermometer; (E) stirrer; (F) subheater; (G) main heater; (H) water cooler; (I) constant temperature bath; (J) N_2 bottle; (K) hand piston; (L, M) quartz pressure transducer; (N) digital pressure indicator; (O) thermometer bridge; (P) voltage/current converter; (Q) PID controller; (R) DC power supply; (S) vacuum pump; (T) variable-volume vessel; (V1) constant volume valve; (V2-V13) valves.

Figure 2. Experimental data distribution of R-125(1) + R-290(2): •, x_1 = 0.000; ◊, x_1 = 0.288; △, x_1 = 0.500; □, x_1 = 0.750; —, vapor pressure curve for R-125; ---, vapor pressure curve for R-290; ×, critical point.

Figure 3. Relative pressure deviations calculated by different models from the present experimental data for pure R-290: •, present model; ◊, REFPROP (ver.6.01)[10]; +, Miyamoto and Watanabe[15].

Figure 4. Relative pressure deviations calculated by different models from the present experimental data for the binary R-125(1) + R-290(2): ◊, this work, x_1 = 0.288; ▲, this work , x_1 = 0.500; ■, this work, x_1 = 0.750; ◊, REFPROP (ver. 6.01)[10], x_1 = 0.288; ▲, REFPROP, x_1 = 0.500; • , REFPROP, x_1 = 0.750.

Figure 5. Temperature dependence of the second virial coefficients of the present model: —, B_{12} this work; —, B_{22} this work; ---, B_{12} this work; +, B_{12}, McElroy[16]; • , B_{22}, McElroy[16].

Figure 6. Temperature dependence of the experimental second virial coefficients for the R-125(1) + R-290(2) system, B_m: •, x_1 = 0.000, i.e., B_{22}; ◊, x_1 = 0.288; △, x_1 = 0.500; • ,

x_1 = 0.750; −, calculated curves by the present model.

Figure 7. Relative deviations of the experimental second virial coefficients, B_m, from the present model: •, x_1 = 0.000, i.e., B_{22}; ◊, x_1 = 0.288; △, x_1 = 0.500; □, x_1 = 0.750.

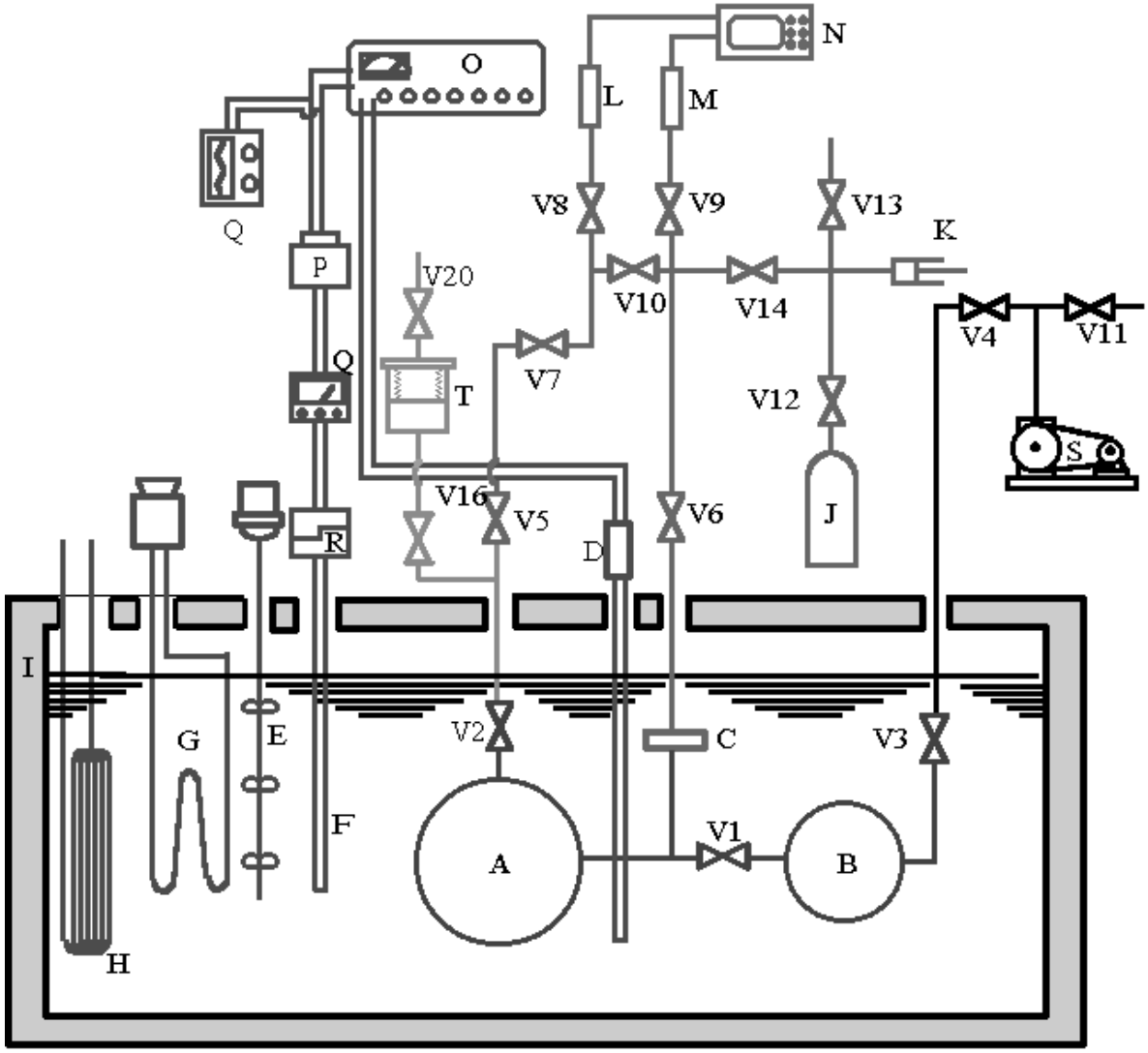

Figure 1. Schematic diagram of the experimental Burnett apparatus: (A) sample cell; (B) expansion cell; (C) differential pressure transducer; (D) platinum resistance thermometer; (E) stirrer; (F) subheater; (G) main heater; (H) water cooler; (I) constant temperature bath; (J) N_2 bottle; (K) hand piston; (L, M) quartz pressure transducer; (N) digital pressure indicator; (O) thermometer bridge; (P) voltage/current converter; (Q) PID controller; (R) DC power supply; (S) vacuum pump; (T) variable-volume vessel; (V1) constant volume valve; (V2-V13) valves.

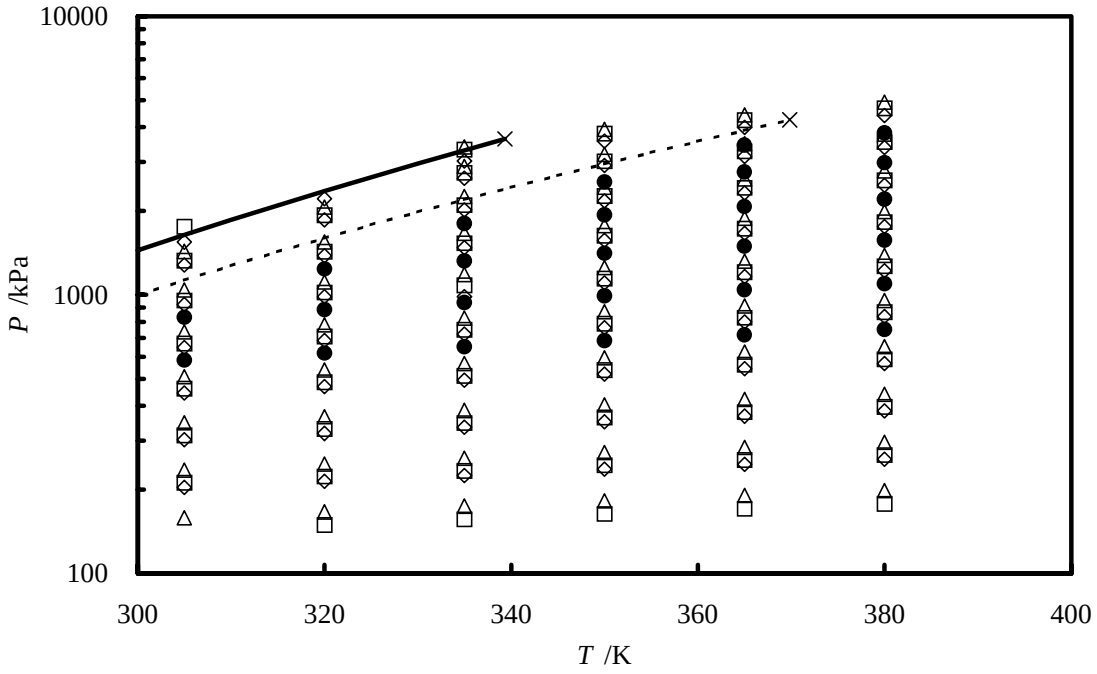

Figure 2. Experimental data distribution of R-125(1) + R-290(2): •, x_1 = 0.000; ◊, x_1 = 0.288; △, x_1 = 0.500; □, x_1 = 0.750; —, vapor pressure curve for R-125; ---, vapor pressure curve for R-290; ×, critical point.

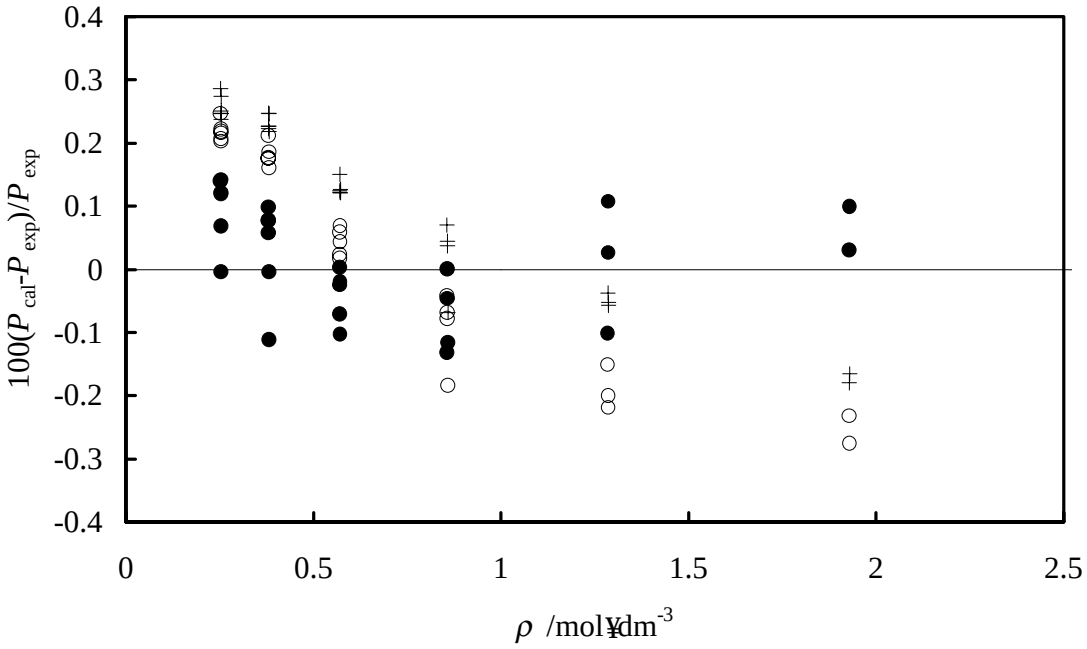

Figure 3. Relative pressure deviations calculated by different models from the present experimental data for pure R-290: •, present model; ◊, REFPROP (ver.6.01)[10]; +, Miyamoto and Watanabe[15].

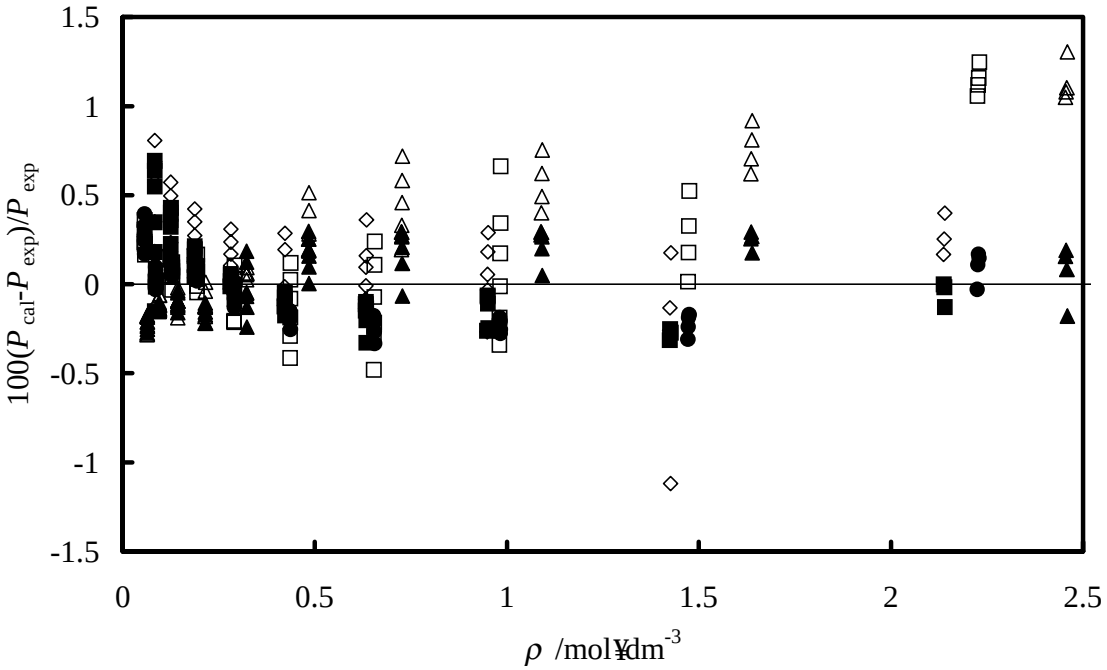

Figure 4. Relative pressure deviations calculated by different models from the present experimental data for the binary R-125(1) + R-290(2): ◇, this work, x_1 = 0.288; ▲, this work , x_1 = 0.500; ■, this work, x_1 = 0.750; ◇, REFPROP (ver. 6.01)[10], x_1 = 0.288; ▲, REFPROP, x_1 = 0.500; ● , REFPROP, x_1 = 0.750.

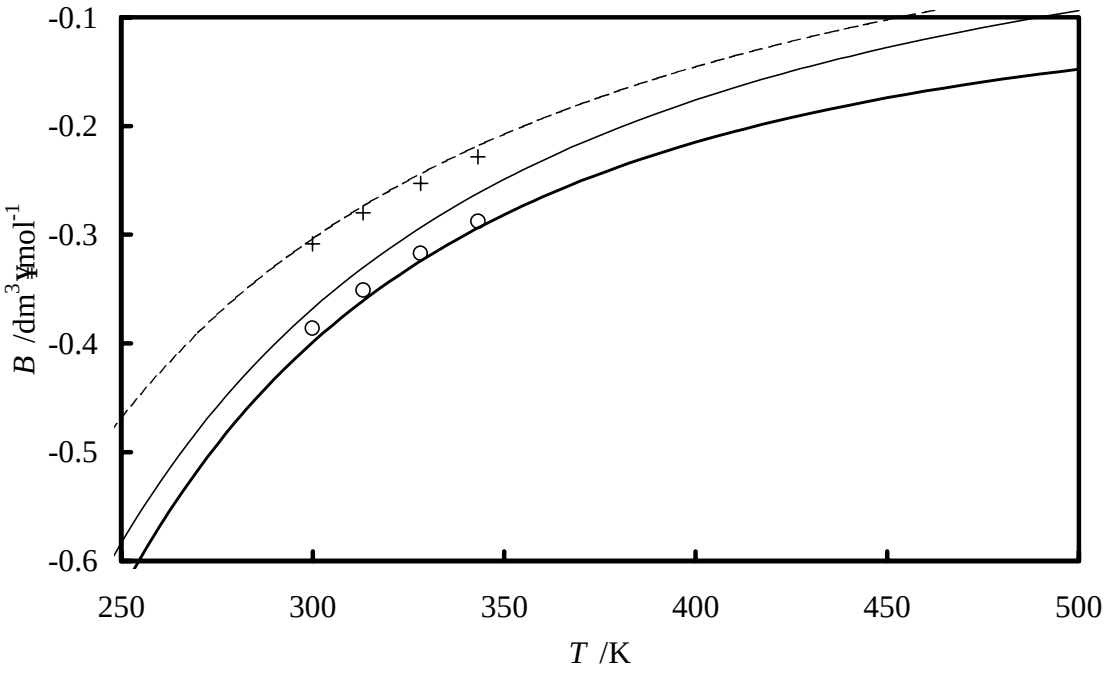

Figure 5. Temperature dependence of the second virial coefficients of the present model: —, B_{12} this work; **—**, B_{22} this work; ---, B_{12} this work; +, B_{12}, McElroy[16]; • , B_{22}, McElroy[16].

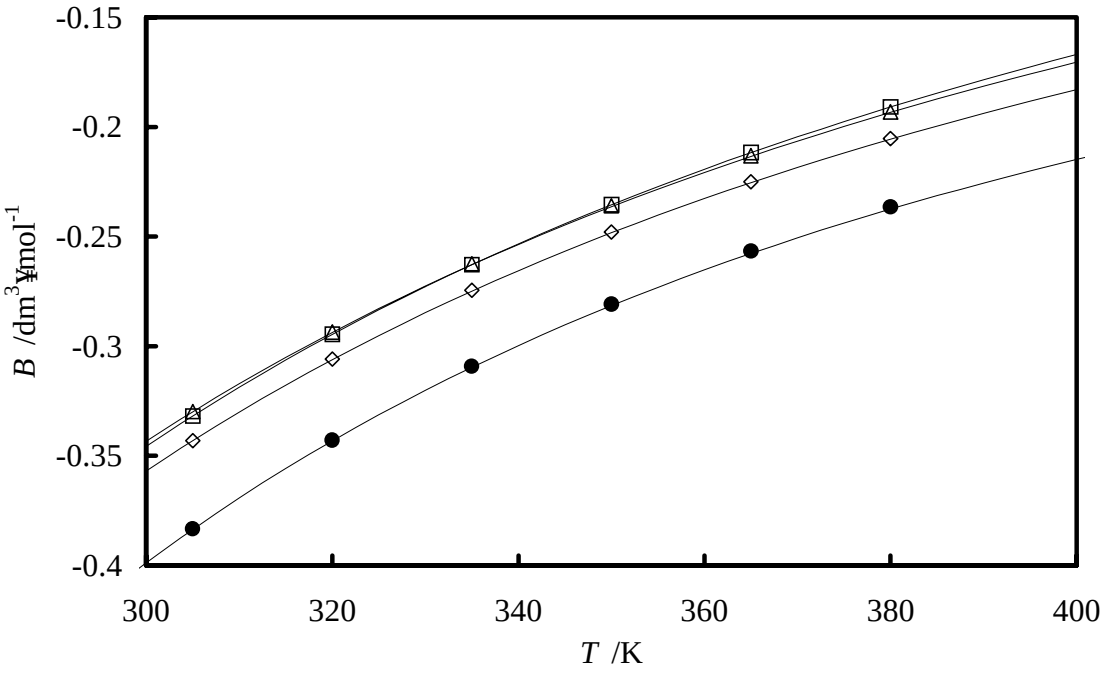

Figure 6. Temperature dependence of the experimental second virial coefficients for the R-125(1) + R-290(2) system, B_m: •, x_1 = 0.000, i.e., B_{22}; ◊, x_1 = 0.288; △, x_1 = 0.500; ·, x_1 = 0.750; —, calculated curves by the present model.

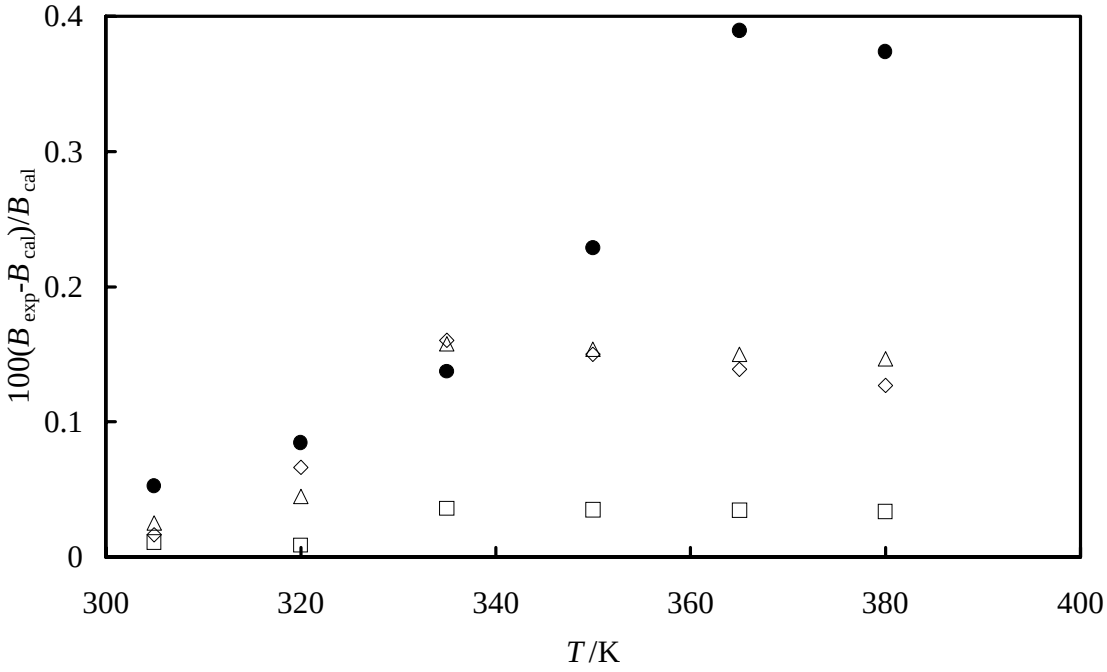

Figure 7. Relative deviations of the experimental second virial coefficients, B_m, from the present model: •, $x_1 = 0.000$, i.e., B_{22}; ◇, $x_1 = 0.288$; △, $x_1 = 0.500$; □, $x_1 = 0.750$.